INTERNATIONAL JOURNAL FOR NUMERICAL METHODS IN FLUIDS
Int. J. Numer. Meth. Fluids 2004; **44**:297–312 (DOI: 10.1002/fld.639)

Newton linearization of the incompressible Navier–Stokes equations

Tony W. H. Sheu*,† and R. K. Lin‡

Department of Engineering Science and Ocean Engineering, National Taiwan University, 73 Chow-Shan Road, Taipei, Taiwan

SUMMARY

The present study aims to accelerate the convergence to incompressible Navier–Stokes solution. For the sake of computational efficiency, Newton linearization of equations is invoked on non-staggered grids to shorten the sequence to the final solution of the non-linear differential system of equations. For the sake of accuracy, the resulting convection–diffusion–reaction finite-difference equation is solved line-by-line using the proposed nodally exact one-dimensional scheme. The matrix size is reduced and, at the same time, the CPU time is considerably saved due to the decrease of stencil points. The effectiveness of the implemented Newton linearization is demonstrated through computational exercises. Copyright © 2004 John Wiley & Sons, Ltd.

KEY WORDS: incompressible; Navier–Stokes solution; non-staggered grids; Newton linearization; convection–diffusion–reaction; nodally exact

1. INTRODUCTION

Numerical simulation of transport equations for momenta in flowing fluids encounters difficulties stemming from approximating multi-dimensional advective flux terms, specifying outflow conditions at truncated boundary and linearizing convective terms in the non-linear momentum equations. Since the way of linearization can significantly affect the rate of convergence towards the final solution, choice of an appropriate linearization method is an important topic in the area of computational fluid dynamics [1].

The simplest and frequently used linearization strategy is to lag the non-linear coefficients shown in the momentum equations. To speed up the convergence, one can simply update the non-linear coefficient. This updating procedure continues until the final steady-state solution to the non-linear equation is obtained. Newton linearization enjoys rapid convergence [2] and

*Correspondence to: Tony W. H. Sheu, Department of Engineering Science and Ocean Engineering, National Taiwan University, 73 Chow-Shan Road, Taipei, Taiwan.
†E-mail: twhsheu@ccms.ntu.edu.tw
‡Ph.D. Candidate.

Contract/grant sponsor: National Science Council; contract/grant number: 90-2811-E-002-008

Received 27 May 2002
Revised 14 April 2003

has been successfully applied to solve for non-linear equations for fluid dynamics and heat transfer. In Newton's method, equation $\mathbf{A}\underline{x} = \underline{b}$, where $\underline{x}$ is the state vector and $\mathbf{A}$ is a function of $\underline{x}$, is approximated by a first-order Taylor series to render $\mathbf{J}\delta\underline{x} = \underline{R}$. Here, the component of the Jacobian matrix (or the Fre'chlet derivative of $\underline{R}$ [3]) is defined by $\mathbf{J}(i,j) = -\partial\underline{R}(i)/\partial x(j)$, where $\underline{R}$ is known as the residual vector $\underline{R} = \underline{b} - \mathbf{A}\underline{x}$. The matrix equation is then solved for $\delta\underline{x}^k$ from $\mathbf{J}\delta\underline{x}^k = \underline{R}^k$, followed by obtaining $\underline{x}^{k+1} = \underline{x}^k + \delta\underline{x}^k$. This is done until the residual norm falls below a user's specified tolerance, with $\mathbf{J}$ and $\underline{R}$ being computed each time using the mostly updated solution $\underline{x}$. Some practical issues of inverting the huge Jacobian matrix $\mathbf{J}$ were discussed in [4].

Newton's method is potentially attractive in accelerating convergence due to its ability to offer q-quadratic convergence [2]. The implementation of this method involves, however, time-consuming manipulation of the Fre'chlet derivative of $\underline{R}$ at the current solution vector $\underline{x}^k$. This disadvantage has been addressed previously by Hunt [5] in his three-dimensional viscous flow analysis. The Newton–Krylov method was proposed to avoid calculation and, thus, storage of the Fre'chlet derivative [3]. The underlying principle of this method is to minimize the residual in a Krylov space by linearizing the equation using the Newton method and solve the resulting linear system of algebraic equations with a Krylov method. Both Arnoldi- and Lanczos-based iterative matrix solution solvers can, thus, be applied [6]. Since the Jacobian matrix is neither formed nor stored, the Newton–Krylov method can be specifically refereed to as a matrix-free Newton–Krylov method [7]. An assessment study of several matrix-free Newton–Krylov methods can be seen in the work of McHugh and Knoll [8]. For a further minimization of residual, a multigrid preconditioner can be used together with the Newton–Krylov linearization procedure [7].

Another major challenge in using Newton's method, assuming the required memory is available, is the increasing radius of convergence. The variable secant procedure, known more generally as the Newton–Raphson method, was proposed to overcome this difficulty by replacing the derivative with a secant line through two points. This potentially attractive linearization method, however, requires factorization of tangent matrix at each iteration [9]. In fact, the need to solve a large-scale system of linear equations at each iteration is considered as a major shortcoming of the Newton-family methods. To reduce memory requirement and computational cost when performing a classical Newton–Raphson linearization method, one can introduce some iterative means to approximately solve the linear system of Newton linearization equations. We refer to this class of methods as the inexact Newton methods [10–12]. In the modified Newton–Raphson method, the tangent matrix is factorized only once for a number of steps. This occasionally updating strategy may lead to poor convergence for a highly non-linear system. As a means of partly circumventing this problem, the asymptotic Newton method was proposed [9]. The Newton-relaxation method [13], with Newton being the primary iteration and relaxation the secondary iteration, is another useful method to avoid direct solution of a large-scale linear system of three-dimensional equations, which must be solved at each iteration of Newton's method. In the light of the above literature survey, Newton's linearization procedure which is suited to be used together with the discretization scheme and the solution algorithm is proposed.

The rest of this paper is organized as follows. In Section 2 the Newton linearization procedure, used together with the iterative solution algorithm, is detailed. This is followed by proposing a discretization scheme mostly suited for solving the resulting linearized momentum equations. Discretization of incompressible Navier–Stokes equations on non-staggered grids is

derailed in Section 4. An assessment study on the present method and the simple iterative update coefficient method is given in Section 5. The last section provides the concluding remarks.

2. LINEARIZATION OF NAVIER–STOKES EQUATIONS

We consider in the paper a two-dimensional steady-state flow equations. Subject to the incompressible constraint condition, the transport equations for the viscous fluid flow in Ω are as follows:

$$u_x + v_y = 0 \tag{1}$$

$$uu_x + vu_y = -p_x + \mu(u_{xx} + u_{yy}) \tag{2}$$

$$uv_x + vv_y = -p_y + \mu(v_{xx} + v_{yy}) \tag{3}$$

In this paper, the subscript denotes the partial derivative. Here, $\underline{\mathbf{u}} = (u, v)$ and p are velocity vector and pressure, respectively. Note that Equations (2) and (3) serve as the transport equations for u and v, respectively. Working equation for p can be obtained as follows by summing the $\partial/\partial x$ (2) and $\partial/\partial y$ (3) and employing (1):

$$p_{xx} + p_{yy} = -[(u_x)^2 + 2u_y v_x + (v_y)^2] \tag{4}$$

Note that the inaccuracy stemming from approximation of terms shown in the right-hand side of (4) for a given velocity field may limit the convergence rate, as discussed [14]. The above pressure Poisson equation needs to be supplemented by the boundary condition given by

$$p_n = [-(\underline{\mathbf{u}} \cdot \nabla)\underline{\mathbf{u}} + \mu\nabla^2\underline{\mathbf{u}} + \underline{\mathbf{f}}] \cdot \underline{\mathbf{n}} \tag{5}$$

where $\underline{\mathbf{n}}$ is the outward-directed unit vector normal to the boundary of Ω. In what follows the dynamic viscosity of the fluid flow is considered uniform for simplicity.

Linearization of convective terms on the left-hand sides of momentum equations (2) and (3) starts from rewriting them as

$$(u^2)_x + (uv)_y = -p_x + \mu(u_{xx} + u_{yy}) \tag{6}$$

$$(uv)_x + (v^2)_y = -p_y + \mu(v_{xx} + v_{yy}) \tag{7}$$

Consider a function st, we can expand it in a Taylor series about the current value and terminate the series expansion after the first-derivative terms. The result is as follows:

$$\begin{aligned} s^{k+1}t^{k+1} &= s^k t^k + \left[\frac{\partial}{\partial s}(st)^k\right](s^{k+1} - s^k) + \left[\frac{\partial}{\partial t}(st)^k\right](t^{k+1} - t^k) + \text{H.O.T} \\ &= s^{k+1}t^k + s^k t^{k+1} - s^k t^k + \text{H.O.T} \end{aligned} \tag{8}$$

In the derivation that follows, all variables denoted by the superscript k are evaluated using solutions obtained at the previous iteration counter. As for terms with the superscript $k+1$, they are evaluated at the most updated iteration and are, therefore, referred to as the active quantities. According to Equation (8), we can linearize $(u^2)_x^{k+1}$ and $(uv)_y^{k+1}$ as

$$\begin{aligned}(u^2)_x^{k+1} &= (u^{k+1}u^k + u^k u^{k+1} - u^k u^k)_x \\ &= u_x^{k+1}u^k + \underline{u^{k+1}u_x^k} + u_x^k u^{k+1} + \underline{u^k u_x^{k+1}} - u_x^k u^k - \underline{u^k u_x^k}\end{aligned} \tag{9a}$$

$$\begin{aligned}(uv)_y^{k+1} &= (u^{k+1}v^k + u^k v^{k+1} - u^k v^k)_y \\ &= u_y^{k+1}v^k + \underline{u^{k+1}v_y^k} + u_y^k v^{k+1} + \underline{u^k v_y^{k+1}} - u_y^k v^k - \underline{u^k v_y^k}\end{aligned} \tag{9b}$$

Substituting (9a) and (9b) into (6) led us to derive the linearized x-momentum equation as follows:

$$\begin{aligned}&u^k u_x^{k+1} + v^k u_y^{k+1} - \mu(u_{xx}^{k+1} + u_{yy}^{k+1}) + \underline{u_x^k u^{k+1}} \\ &= -p_x^{k+1} + \underline{u^k u_x^k + v^k u_y^k - u_y^k v^{k+1}}\end{aligned} \tag{10}$$

Similarly, one can derive the following convection–diffusion–reaction (CDR) equation for v

$$\begin{aligned}&u^k v_x^{k+1} + v^k v_y^{k+1} - \mu(v_{xx}^{k+1} + v_{yy}^{k+1}) + \underline{v_y^k v^{k+1}} \\ &= -p_y^{k+1} + \underline{u^k v_x^k + v^k v_y^k - v_x^k u^{k+1}}\end{aligned} \tag{11}$$

Neglect of the underlined terms from the Newton linearization Equations (10) and (11) results in the conventional lagging coefficient linearized equations.

For computational efficiency, we can solve for Equation (10), for example, iteratively by virtue of the following Alternating Direction Implicit (ADI) steps [15]:

$$u^k u_x^{k+1} - \mu u_{xx}^{k+1} + u_x^k u^{k+1} = -p_x^{k+1} + v^k u_y^{k+1} - \mu u_{yy}^{k+1} + f_1 \tag{12a}$$

$$v^k u_y^{k+1} - \mu u_{yy}^{k+1} + u_x^k u^{k+1} = -p_x^{k+1} + u^k u_x^{k+1} - \mu u_{xx}^{k+1} + f_2 \tag{12b}$$

where

$$f_1 = u^k u_x^k + v^k u_y^k - u_y^k v^{k+1} \tag{13a}$$

$$f_2 = u^k u_x^k + v^k u_y^k - u_y^k v^{k+1} \tag{13b}$$

Note that when an ADI method is applied together with the pseudo-transient approach, where pseudo-time derivative terms are added to the steady Navier–Stokes equations so as to be able to parabolize the elliptic differential system for time marching, its strong convergence property discussed in Reference [16] deteriorates considerably for cases involving complex geometries and high Reynolds numbers [17]. Under these circumstances, use of an ADI method is constrained by a small time increment to maintain convergence solutions to steady-state.

3. NUMERICAL MODEL

As Equations (12a) and (12b) show, the prototype equation takes the following form:

$$u\Phi_x + v\Phi_y - k(\Phi_{xx} + \Phi_{yy}) + c\Phi = f \tag{14}$$

For simplicity, the model equation is solved subject to a specified boundary value of Φ. In the above, k and c denote the diffusion coefficient and the reaction coefficient, respectively. In what follows u, v, k and c are assumed to have constant values.

By virtue of the operator splitting method of Peaceman and Rachford [15], solutions to Equation (14) are sought from the predictor and corrector steps, respectively:

$$u\Phi_x^* - k\Phi_{xx}^* + c\Phi^* = f_1 \tag{15a}$$

$$v\Phi_y^{n+1} - k\Phi_{yy}^{n+1} + c\Phi^{n+1} = f_2 \tag{15b}$$

In the above, $f_1 = f^* - v\Phi_y^n - k\Phi_{yy}^n$ and $f_2 = f^{n+1} - u\Phi_x^* - k\Phi_{xx}^*$. As Equations (15a) and (15b) reveal, a key concern in the analysis of the two-dimensional CDR equation (14) is the discretization of the following one-dimensional equation:

$$u\Phi_x - k\Phi_{xx} + c\Phi = f \tag{15c}$$

For illustrative purposes, f is assumed to be a known constant.

Our strategy of approximating (15c) is to employ its general solution

$$\Phi = c_1 e^{\lambda_1 x} + c_2 e^{\lambda_2 x} + \frac{f}{c} \tag{16}$$

where $(\lambda_1, \lambda_2) = (u + \sqrt{u^2 + 4ck}/2k, u - \sqrt{u^2 + 4ck}/2k)$. In Equation (16), c_1 and c_2 are constants. Terms other than the diffusive term shown in Equation (15c) are approximated by the centre-like scheme. Therefore, the discrete equation at an interior node i can be expressed as

$$\left(-\frac{u}{2h} - \frac{m}{h^2} + \frac{c}{6}\right)\Phi_{i-1} + 2\left(\frac{m}{h^2} + \frac{c}{3}\right)\Phi_i + \left(\frac{u}{2h} - \frac{m}{h^2} + \frac{c}{6}\right)\Phi_{i+1} = f \tag{17}$$

where h is the mesh size. We then substitute the exact solutions $\Phi_i = c_1 e^{\lambda_1 x_i} + c_2 e^{\lambda_2 x_i} + f/c$, $\Phi_{i+1} = c_1 e^{\lambda_1 h} e^{\lambda_1 x_i} + c_2 e^{\lambda_2 h} e^{\lambda_2 x_i} + f/c$, and $\Phi_{i-1} = c_1 e^{-\lambda_1 h} e^{\lambda_1 x_i} + c_2 e^{-\lambda_2 h} e^{\lambda_2 x_i} + f/c$ into Equation (17).

The closed-form of m can be derived as [18]

$$m = h^2 \left\{ \frac{c/3 + c/6\cosh(\overline{\lambda_1})\cosh(\overline{\lambda_2}) + u/2h\sinh(\overline{\lambda_1})\cosh(\overline{\lambda_2})}{\cosh(\overline{\lambda_1})\cosh(\overline{\lambda_2}) - 1} \right\} \tag{18}$$

where $(\overline{\lambda_1}, \overline{\lambda_2}) = (uh/2k, \sqrt{(uh/2k)^2 + ch^2/k})$. Note that the predicted inaccuracy stems solely from the approximated f.

4. INCOMPRESSIBLE NAVIER–STOKES CALCULATION ON NON-STAGGERED GRIDS

On physical grounds, $-\nabla p$ in the equations of motion is discretized by a centred scheme. However, centre approximation of $\partial p/\partial x$ and $\partial p/\partial y$ on non-staggered grids engenders spurious even–odd oscillations [19, 20]. Therefore, one has to suppress these erroneous checkerboarding pressures when simulating the incompressible flow equations on grids of the simplest form [21].

For overcoming difficulty with the even–odd decoupling, we calculate $F_j(\equiv h\Phi_x)$ and $G_j(\equiv h^2\Phi_{xx})$ implicitly from

$$\begin{aligned} \alpha_0 F_{j+1} + \beta_0 F_j + \gamma_0 F_{j-1} = {} & a_0(\Phi_{j+2} - \Phi_{j+1}) + b_0(\Phi_{j+1} - \Phi_j) \\ & + c_0(\Phi_j - \Phi_{j-1}) + d_0(\Phi_{j-1} - \Phi_{j-2}) \end{aligned} \tag{19}$$

and

$$\alpha_1 G_{j+1} + \beta_1 G_j + \gamma_1 G_{j-1} = a_1\Phi_{j+2} + b_1\Phi_{j+1} + c_1\Phi_j + d_1\Phi_{j-1} + e_1\Phi_{j-2} \tag{20}$$

Provided that $(\alpha_0, \beta_0, \gamma_0, a_0, b_0, c_0, d_0) = (\frac{1}{5}, \frac{3}{5}, \frac{1}{5}, \frac{1}{60}, \frac{29}{60}, \frac{29}{60}, \frac{1}{60})$ and $(\alpha_1, \beta_1, \gamma_1, a_1, b_1, c_1, d_1, e_1) = (1, \frac{11}{2}, 1, \frac{3}{8}, 6, -\frac{51}{4}, 6, \frac{3}{8})$, both Φ_x and Φ_{xx} accommodate sixth-order accuracy.

The implicit equations for F and G at nodes immediately adjacent to the boundary can be derived by specifying $d_0 = e_1 = 0$ and $a_0 = a_1 = 0$ at nodes next to the left and right boundaries, respectively. By performing Taylor series expansion, the coefficients can be analytically derived as $(\alpha_0, \beta_0, \gamma_0, a_0, b_0, c_0, d_0) = (\frac{3}{10}, \frac{3}{5}, \frac{1}{10}, \frac{1}{30}, \frac{19}{30}, \frac{1}{3}, 0)$ and $(\frac{1}{10}, \frac{3}{5}, \frac{3}{10}, 0, \frac{1}{3}, \frac{19}{30}, \frac{1}{30})$ at nodes next to the left and right boundaries, respectively. In addition, coefficients for evaluating G_j are exactly derived as $(\alpha_1, \beta_1, \gamma_1, a_1, b_1, c_1, d_1, e_1) = (1, 10, 1, 0, 12, -24, 12, 0)$.

5. NUMERICAL RESULTS

5.1. Non-linear advection–diffusion scalar equation

To verify the proposed Newton linearization method, the following two-dimensional non-linear convection–diffusion equation for u is considered in $0 \leqslant x, y \leqslant 1$:

$$uu_x + vu_y - k(u_{xx} + u_{yy}) = f \tag{21}$$

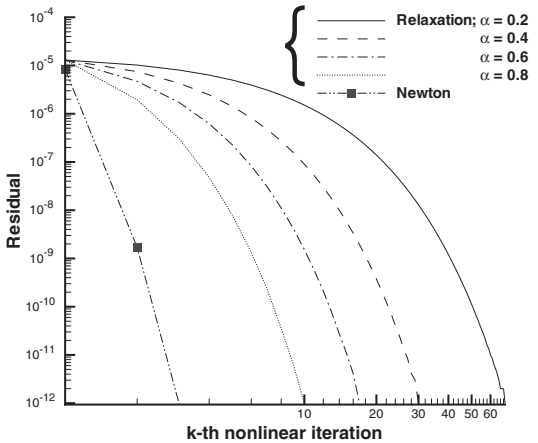

Figure 1. Comparison of the convergence histories, with the initial guess value $u = 0.5$, for solving the non-linear advection–diffusion equation (21).

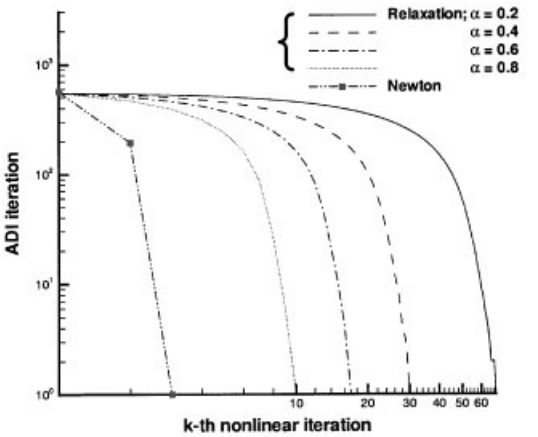

Figure 2. Plots of the ADI iteration number against the outer (non-linear) iteration number for the two investigated linearization methods.

The validation test was performed at $k = x^2$, $v = y$ and $f = 2x^3(y^4 - x)$. The solution to equation (21) was exactly derived as $u = x^2 y^2$.

We assess our proposed model and then the standard relaxation method based on $\underline{\mathbf{u}}^{\text{new}} = \alpha\underline{\mathbf{u}}^{\text{new}} + (1-\alpha)\underline{\mathbf{u}}^{\text{old}}$, where $0 \leqslant \alpha \leqslant 1$. As Figure 1 shows, a considerable amount of non-linear iterations has been saved in view of the iteration numbers needed for the results obtained at $\alpha = 0.2$, 0.4, 0.6 and 0.8. The tolerance, defined as $[1/\mathbf{N}\sum(\underline{\mathbf{u}}^{\text{new}} - \underline{\mathbf{u}}^{\text{old}})^2]^{1/2}$, set for each calculation is 10^{-13}. Here, $\mathbf{N}$ denotes the number of solution points. We also compare the iteration numbers needed to reach the convergent ADI solution at each non-linear iteration. It is seen from Figure 2 that much fewer ADI iterations are needed when using the present Newton linearization method.

5.2. Non-linear Navier–Stokes equations

For the sake of validation, a problem with $\underline{\mathbf{f}} = 0$ is considered. The analytic pressure in the unit square is

$$p = \frac{-2}{(1+x)^2 + (1+y)^2} \tag{22}$$

provided that the boundary velocities are analytically specified as

$$u = \frac{-2(1+y)}{(1+x)^2 + (1+y)^2} \tag{23a}$$

$$v = \frac{2(1+x)}{(1+x)^2 + (1+y)^2} \tag{23b}$$

In Figure 3, we plot the computed rates of convergence for u, v, and p according to

$$\mathbf{C} = \frac{\ln ||err_1|| - \ln ||err_2||}{\ln |h_1| - \ln |h_2|} \tag{24}$$

The error measure is cast in the discrete L_2-norm

$$\mathbf{E} = \left[\frac{1}{\mathbf{M}} \sum_{i,j=1}^{\mathbf{M}^{1/2}} (\mathbf{u}_{ij} - \mathbf{U}_{ij})^2 \right]^{1/2} \tag{25}$$

In the above equation, $\mathbf{U}_{ij}$ denotes the exact solution at an interior nodal point (i, j) and $\mathbf{u}_{ij}$ is the corresponding finite-difference solution. As the computed rates of convergence show in Figure 3, the validity of the method is justified. Like the scalar problem, it is found that

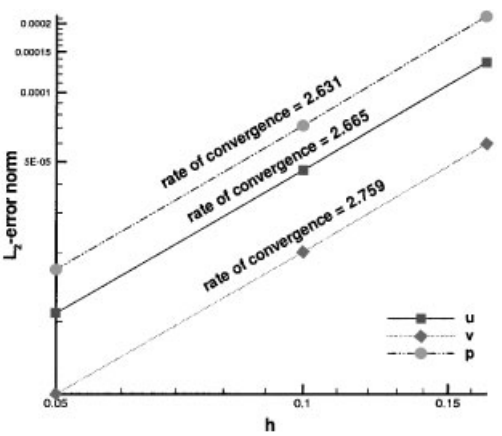

Figure 3. The computed rates of convergence for u, v and p.

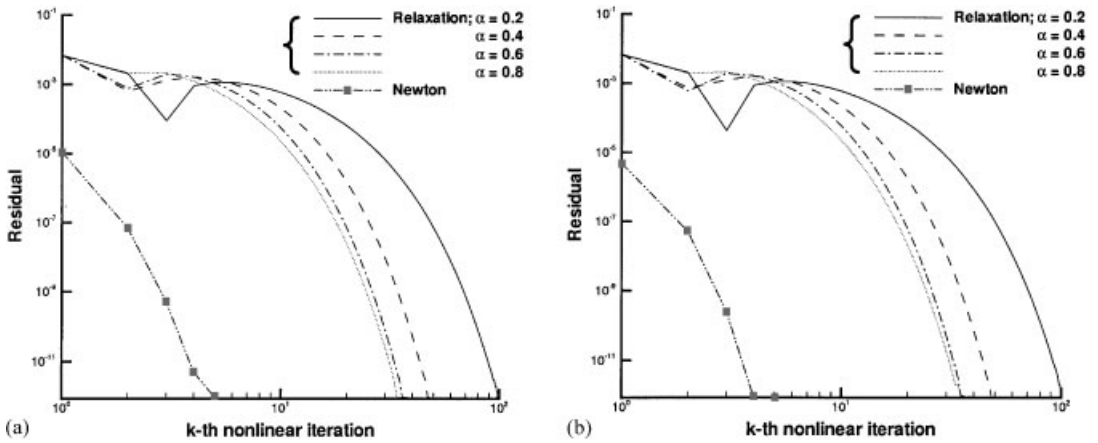

Figure 4. Comparison of the convergent histories for solving the non-linear Navier–Stokes problem, which has the analytic solutions given in (22)–(23b) at $Re = 1000$. The initial guess solutions for u and v are $u = v = 0.5$: (a) convergence histories for u; and (b) convergence histories for v.

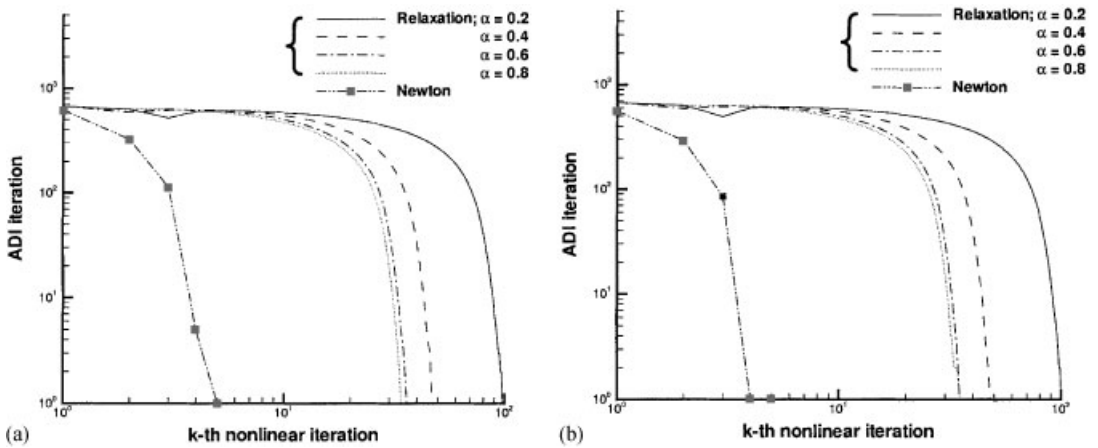

Figure 5. Plots of the ADI iteration number against the outer (non-linear) iteration number for the two investigated linearization methods: (a) u; and (b) v.

a considerable amount of non-linear and ADI iterations can be saved, as seen in Figures 4 and 5.

The second problem to be investigated is known as the Kovasznay flow problem [22], which is amenable to the analytic solutions given below

$$u = 1 - e^{\lambda x} \cos(2\pi y) \tag{26a}$$

$$v = \frac{\lambda}{2\pi} e^{\lambda x} \sin(2\pi y) \tag{26b}$$

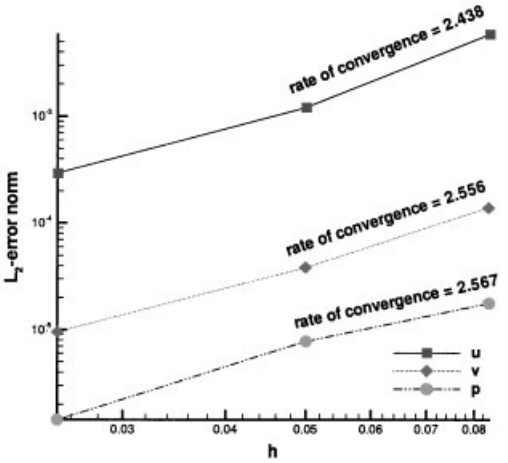

Figure 6. The computed rates of convergence for u, v and p.

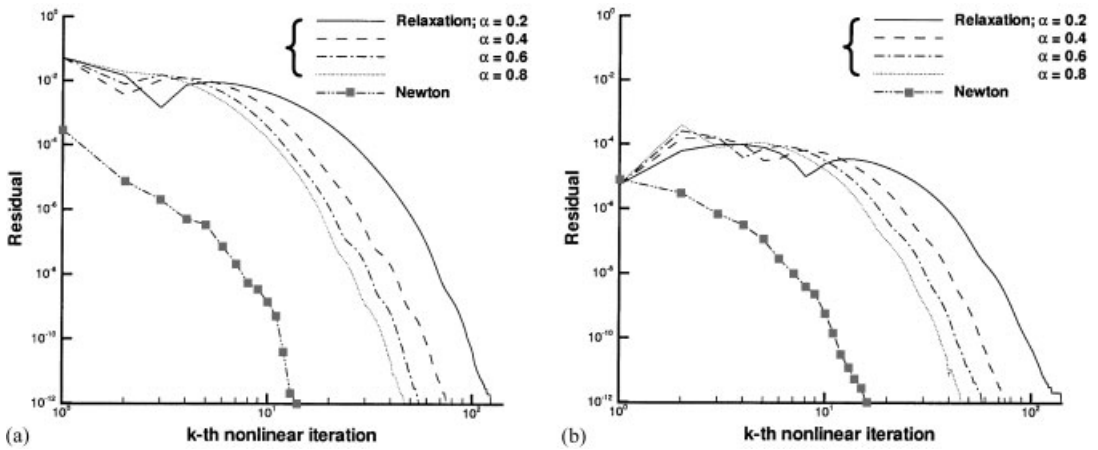

Figure 7. Comparison of the convergent histories for solving the non-linear Navier–Stokes problem, which has the analytic solutions given in (27) at $Re = 1000$. The initial guess solutions for u and v are $u = v = 0.5$: (a) convergence histories for u; and (b) convergence histories for v.

$$p = \frac{1}{2}(1 - \mathrm{e}^{2\lambda x}) \tag{26c}$$

where $\lambda = Re/2 - (Re^2/4 + 4\pi^2)^{1/2}$. Numerical calculations have been carried out in a square which is covered with uniform grids. For the test Reynolds number 1000, both pressure and velocity fields are well-predicted, as seen from the predicted errors shown in Figure 6. As the error reduction plot shows in Figure 7, non-linear iteration numbers have been considerably saved. The inner iteration number for each non-linear iteration is also largely reduced, as seen in Figure 8. This clearly shows the advantage of using the Newton linearization method.

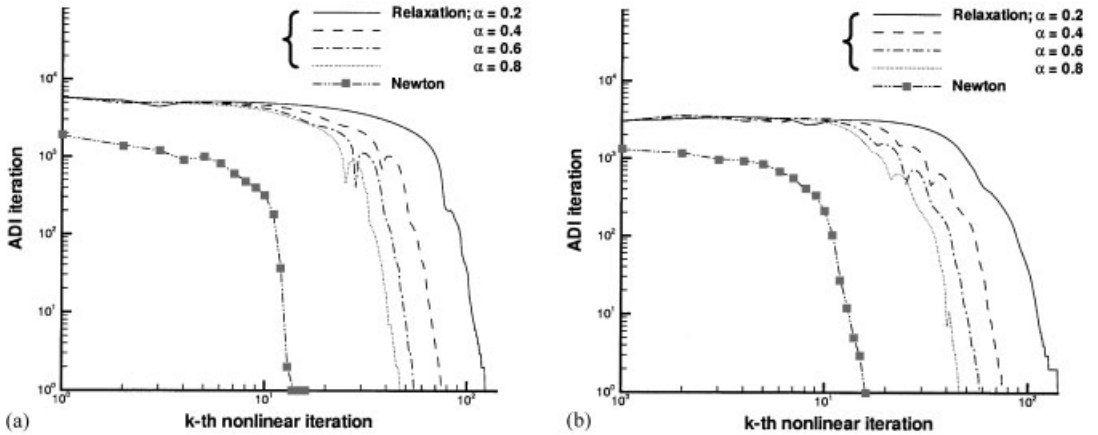

Figure 8. Plots of the ADI iteration number against the outer (non-linear) iteration number for the two investigated linearization methods: (a) u; and (b) v.

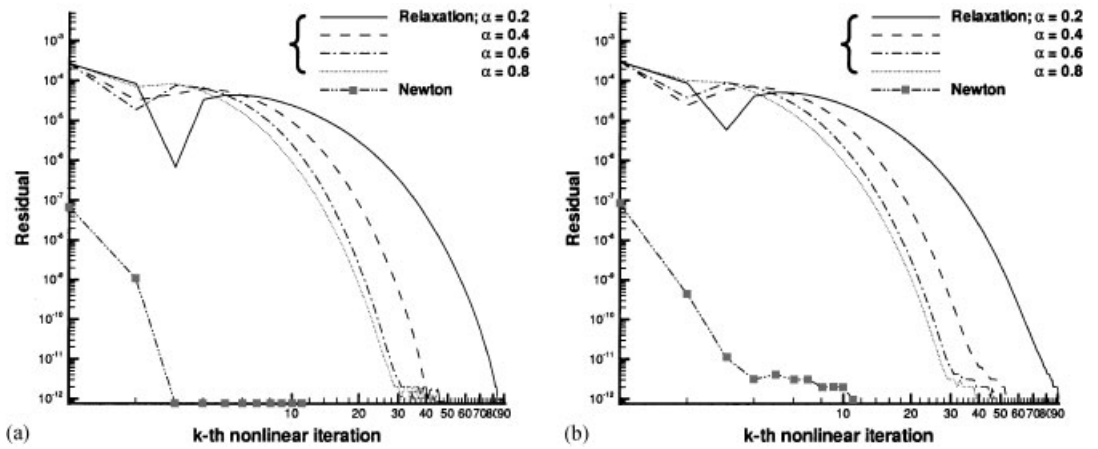

Figure 9. Comparison of the convergent histories for solving the non-linear Navier–Stokes problem, which has the analytic solutions given in (28)–(30) at $Re = 1000$. The initial guess solutions for u and v are $\underline{\mathbf{u}} = 0.5$: (a) convergence histories for u; and (b) convergence histories for v.

The validation and assessment are followed by considering another analytic lid-driven cavity flow problem [23]. In a square domain, the Navier–Stokes equations are solved subject to the following boundary conditions for u and v at $x = 0,\ 1$ and $y = 0,\ 1$:

$$u = 8(x^4 - 2x^3 + x^2)(4y^3 - 2y) \tag{27a}$$

$$v = -8(4x^3 - 6x^2 + 2x)(y^4 - y^2) \tag{27b}$$

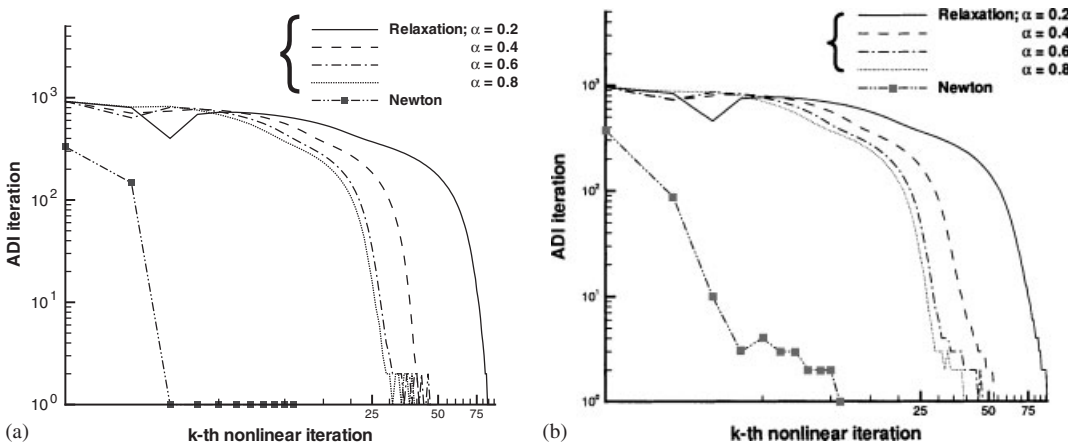

Figure 10. Plots of the ADI iteration number against the outer (non-linear) iteration number for the two investigated linearization methods: (a) u; and (b) v.

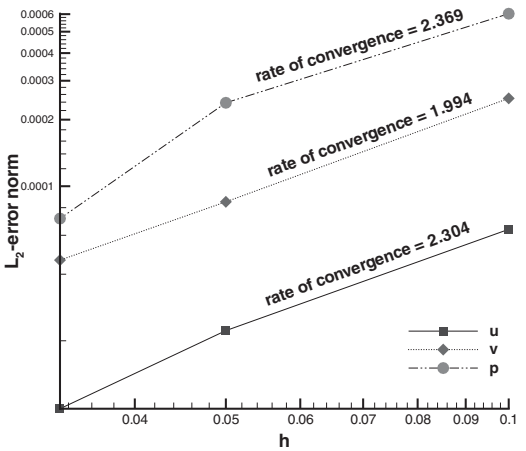

Figure 11. The computed rates of convergence for u, v and p.

Moreover, as the body force $\underline{\mathbf{f}} = (f_1, f_2)$ is given as

$$f_1 = 0 \tag{28a}$$

$$f_2 = \frac{Re}{8}[24J_1(x) + 2I_1'(x)I_2''(y) + I_1'''(x)I_2(y)] + 64[J_3(x)J_4(y) - I_2(y)I_2'(y)J_2(x)] \tag{28b}$$

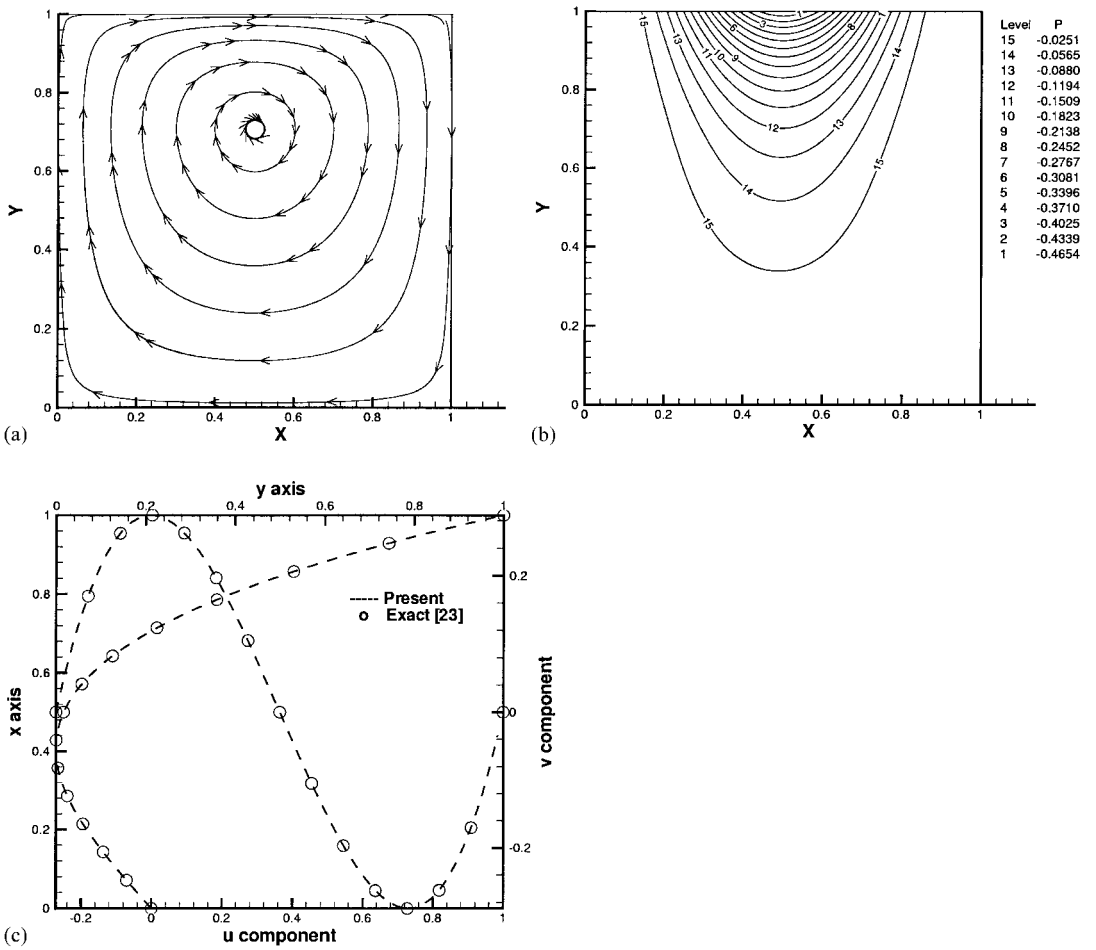

Figure 12. The computed solutions at $Re = 1000$: (a) streamlines; (b) pressure contours; and (c) mid-sectional velocity profiles for u and v.

the pressure solution takes the following analytic form:

$$p = \frac{8}{Re}[J_1(x)I_2'''(y) + I_1'(x)I_2'(y)] + 64J_3(x)[I_2(y)I_2''(y) - (I_2'(y))^2] \tag{29}$$

where

$$I_1(x) = x^4 - 2x^3 + x^2$$

$$I_2(y) = y^4 - y^2$$

$$J_1(x) = 0.2x^5 - 0.5x^4 + \tfrac{1}{3}x^3$$

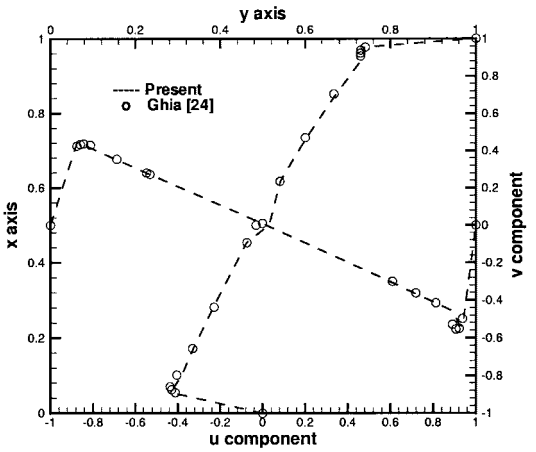

Figure 13. A comparison of the computed and Ghia's velocity profiles for $u(x, 0.5)$ and $v(0.5, y)$ at $Re = 5000$.

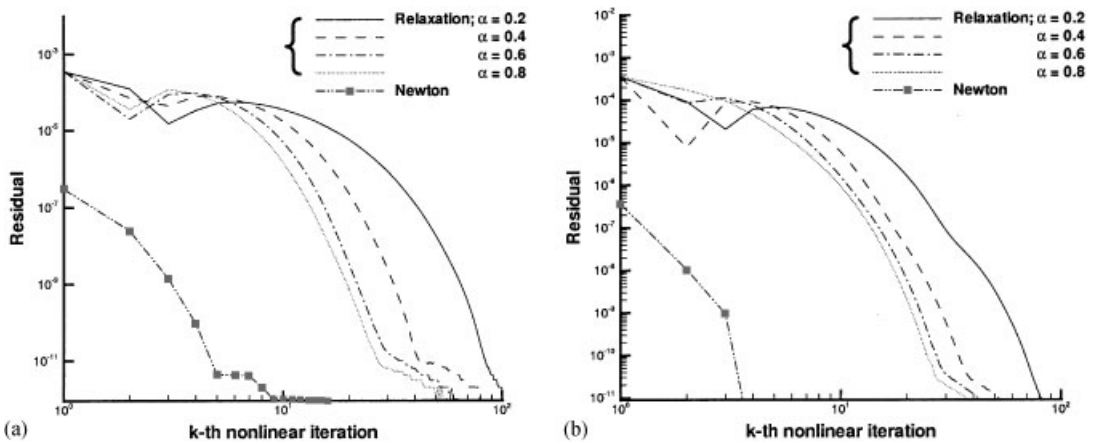

Figure 14. Comparison of the convergent histories for solving the lid-driven cavity flow problem at $Re = 5000$. The initial guess solutions for u and v are $u = v = 0.5$: (a) convergence histories for u; and (b) convergence histories for v.

$$J_2(x) = -4x^6 + 12x^5 - 14x^4 + 8x^3 - 2x^2$$

$$J_3(x) = 0.5(x^4 - 2x^3 + x^2)^2$$

$$J_4(y) = -24y^5 + 8y^3 - 4y$$

Considering the case with $Re = 1000$, employment of the Newton linearization method renders a much faster convergent solution. The evidences are given in Figures 9 and 10,

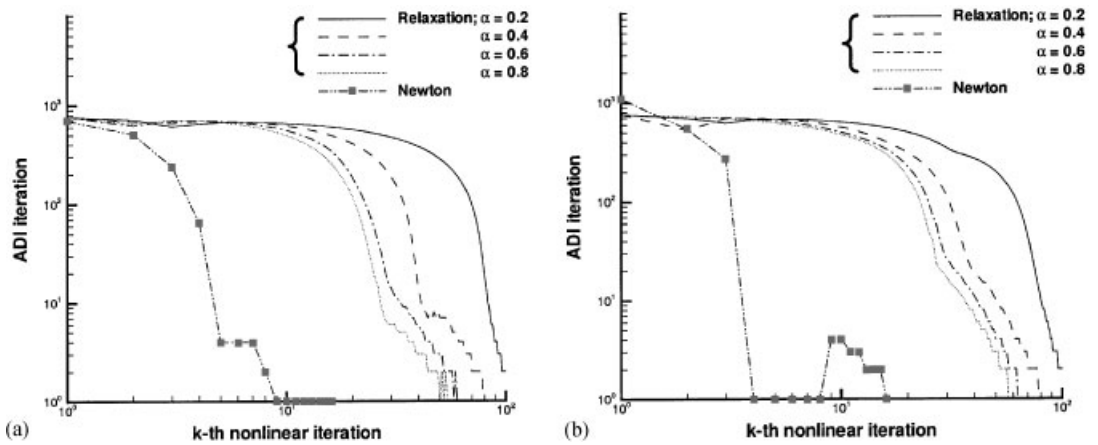

Figure 15. Plots of the ADI iteration number against the outer (non-linear) iteration number for the two investigated linearization methods: (a) u; and (b) v.

from which a considerable amount of CPU time is saved. The computed solutions given in Figure 11 reveal that the proposed model offers good accuracy but not at the cost of deteriorated convergence. For completeness, the contour levels for streamline and pressure are plotted in Figure 12, together with the mid-sectional velocity profiles for u and v.

5.3. *Lid-driven cavity flow problem*

The next Navier–Stokes problem considers the cavity flow driven by a constant upper lid velocity u_{lid}. The geometrical simplicity and physical complexity have made this problem an attractive test for benchmarking the incompressible Navier–Stokes models. With ℓ as the characteristic length, u_{lid} the characteristic velocity, the Reynolds number under investigation is 5000.

We continuously refine the mesh and plot the grid independent mid-plane velocity profiles $u(0.5, y)$ and $v(x, 0.5)$ in Figure 13. For the sake of comparison, the steady-state benchmark solutions obtained by Ghia [24] are also given in the same figure. The agreement between the two numerical solutions is extremely good. Most importantly, much improved convergence histories are seen from Figures 14 and 15 and these confirm the applicability of the proposed scheme.

6. CONCLUDING REMARKS

The objective of this study is to show the effectiveness of using the Newton linearization method to solve for the incompressible Navier–Stokes equations. Revealed from this study is that the linearized equations can be efficiently solved on non-staggered grids using the computationally very accurate CDR scheme. Numerical study of several problems shows the effectiveness of Newton's method in offering much faster outer iteration (or non-linear iteration) and inner iteration (ADI iteration) convergence to the convergent solutions is seen for all test problems.

ACKNOWLEDGEMENTS

We acknowledge the financial support from National Science Council under NSC 90-2811-E-002-008. This work was partially accomplished in the course of the first author's sabbatical leave in University of Paris 6. The facilities provided by Professors Oliver Pironneau and Yvon Maday are highly appreciated. A list of useful references suggested by the anonymous reviewer is gratefully acknowledged.

REFERENCES

1. Galpin PF, Raithby GD. Treatment of non-linearities in the numerical solution of the incompressible Navier–Stokes equations. *International Journal for Numerical Methods in Fluids* 1986; **6**:409–426.
2. Dennis Jr JE, Schmabel RB. *Numerical Methods for Unconstrained Optimization and Nonlinear Equations*. Prentice-Hall: Englewood Cliffs, NJ, 1983.
3. Pereira JMC, Kobayahi MH, Pereira JCF. A fourth-order-accurate finite volume compact method for the incompressible Navier–Stokes solutions. *Journal of Computational Physics* 2001; **167**:217–243.
4. Hunt R. The numerical solution of the flow in a general bifurcating channel at moderately high Reynolds number using boundary-filed co-ordinates, primitive variables and Newton iteration. *International Journal for Numerical Methods in Fluids* 1993; **17**:711–729.
5. Hunt R. Three-dimensional steady flow in a divergent channel using finite and pseudo spectral differences. *SIAM Journal on Scientific Computing* 1996; **17**(3):561–578.
6. McHugh PR, Knoll DA. Fully coupled finite volume solutions of the incompressible Navier–Stokes and energy equations using an inexact Newton method. *International Journal for Numerical Methods in Fluids* 1994; **19**:439–455.
7. Pernice M, Tocci MD. A multigrid-preconditioned Newton–Krylov method for the incompressible Navier–Stokes equations. *SIAM Journal on Scientific Computing* 2001; **23**(2):398–418.
8. McHugh PR, Knoll DA. Comparison of standard and matrix-free implementations of several Newton–Krylov solvers. *AIAA Journal* 1994; **32**(12):2394–2400.
9. Hadji S, Dhatt G. Asymptotic-Newton method for solving incompressible flows. *International Journal for Numerical Methods in Fluids* 1997; **25**:861–878.
10. Dembo RS, Eisenstat SC, Steihaug T. Inexact Newton methods. *SIAM Journal on Numerical Analysis* 1982; **19**:400–408.
11. Eisenstat SC, Walker HF. Globally convergent inexact Newton methods. *SIAM Journal on Optimization* 1994; **4**:393–422.
12. Eisenstat SC, Walker HF. Choosing the Newton method. *SIAM Journal on Scientific Computing* 1996; **17**: 16–32.
13. Sheng C, Taylor LK, Whitfield DL. Multigrid algorithm for three-dimensional incompressible high-Reynolds number turbulent flows. *AIAA Journal* 1995; **33**(11):2073–2079.
14. Chaviaropoulos P, Giannakoglou K. A vorticity-streamfunction formulation for steady incompressible two-dimensional flows. *International Journal for Numerical Methods in Fluids* 1996; **23**:431–444.
15. Peaceman DW, Rachford HH. The numerical solution of parabolic and elliptic differential equations. *Journal of the Society for Industrial and Applied Mathematics* 1955; **3**:28–41.
16. Stone HL. Iterative solution of implicit approximation of multi-dimensional partial differential equations. *SIAM Journal on Numerical Analysis* 1968; **5**:530–558.
17. Jordan SA. An iterative scheme for numerical solution of steady incompressible viscous flows. *Computers and Fluids* 1992; **21**(4):503–517.
18. Sheu TWH, Wang SK, Lin RK. An implicit scheme for solving the convection–diffusion–reaction equation in two dimensions. *Journal of Computational Physics* 2000; **164**:123–142.
19. Patankar SV. *Numerical Heat Transfer and Fluid Flow*. Hemisphere: New York, 1990.
20. Harlow FW, Welch JE. Numerical calculation of time-dependent viscous incompressible flow of fluid with free surfaces. *The Physics of Fluids* 1965; **8**:2182–2189.
21. Rhie CM, Chow WL. Numerical study of the turbulent flow past an airfoil with trailing edge separation. *AIAA Journal* 1983; **21**:1525–1532.
22. Kovasznay LIG. Laminar flow behind a two-dimensional grid. *Proceedings of Cambridge Philosophical Society* 1948, **44**.
23. Shih TM, Tan CH, Hwang BC. Effects of grid staggering on numerical schemes. *International Journal for Numerical Methods in Fluids* 1989; **8**:193–212.
24. Ghia U, Ghia KN, Shin CT. High-*Re* solutions for incompressible flow using the Navier–Stokes equations and a multigrid method. *Journal of Computational Physics* 1982; **48**:387–411.

